

# Magnetic Nanoparticles: from Synthesis to Theranostics

**Kheireddine El-Boubbou\***

<sup>a</sup>King Saud bin Abdulaziz University for Health Sciences (KSAU-HS), King Abdulaziz Medical City, National Guard Health Affairs, Riyadh 11481, Saudi Arabia

<sup>b</sup>King Abdullah International Medical Research Center (KAIMRC), King Abdulaziz Medical City, Riyadh 11426, Saudi Arabia

**Submission:** March 06, 2017; **Published:** April 05, 2017

**\*Corresponding author:** Kheireddine El-Boubbou, King Saud bin Abdulaziz University for Health Sciences (KSAU-HS), Saudi Arabia, E-mail: elboubboukh@ngha.med.sa; boubbouk@ksau-hs.edu.sa

## Abstract

Magnetic nanoparticles (MNPs), particularly made of iron oxides, hold great promise for biomedical theranostic applications particularly as diagnostic imaging agents and drug delivery carriers. Such potential stems from their unique intrinsic physicochemical and biochemical properties including excellent magneto-responsive properties, low toxicity, colloidal stability, and facile surface engineering capability. Herein, the most prominent synthetic approaches employed for preparation of biocompatible colloidal MNPs utilized for biomedical endpoints are outlined. Particular attention is devoted to the utilization of MNPs as multimodal imaging agents with notable examples presented. Undoubtedly, in the upcoming years, MNP formulations will serve as potentially promising diagnostic and therapeutic candidates in magneto-responsive medical theranostics.

**Keywords:** Magnetic nanoparticles; Iron oxide; Drug delivery; Cancer; Anticancer drugs; Magnetic drug targeting; Diagnosis; Theranostics

## Introduction

“Nanotechnology” refers simply to the chemistry of the “small” –very small where novel and exciting phenomena occur. Nanotechnology, itself, is nothing but an impeccable reflection of the dimensions of nature. The manufacturing and syntheses of certain biomolecules at the atomic and molecular resolution, in a controlled precise manner, is a perfect example of what is today known as nanotechnology [1]. This has continuously inspired scientists to seek innovative methodologies providing nanomaterials with tailored features, novel chemical, and specific optical properties [2]. “Things behave differently or strangely at the nanoscale”-we often hear this phrase, but what does it exactly mean? It has mainly to do with physical and chemical (physicochemical) when materials are so tiny, the electrons become squeezed into space smaller than they prefer leading to confinement effects, thus, higher energies and subsequent astonishing optical and magnetic volume/surface ratio: at the nanoscale, most of the material is surface and very little is volume; smaller things have much more outside (surface) than inside (volume), with more surface leading to more and more space for chemical and conjugation reactions.

Natural processes such as the buildup of self-organized and self-assembled ordered structures have always inspired scientists to look for unique ways to create new micro- and nano- scale objects [3]. The aim is to produce large-scale, carefully arranged nanostructures using simplest procedures on a practical and industrial time-scale. In the last decade, the continuous trials to produce monodisperse, uniform, versatile, stable, and biocompatible magnetic metal oxide nanoparticles (MNPs) for both *in-vitro* and *in-vivo* applications have sky-rocketed [4-7]. Besides their utilization in a variety of physioelectronic applications ranging from information-storage and electronic devices, their use in advanced biomedicine for molecular and cellular magnetic resonance imaging (MRI), as well as drug delivery vehicles for disease theranostics offered such NPs their glow [8-12]. In particular, the use of MNPs made of iron oxides (denoted as MIONPs) for bacterium and cellular detection [13,14], molecular imaging [15-17], and drug delivery systems [18-21] has attracted immense attention. With their spherical shape, nanometer dimensions and large surface area, MIONPs present a powerful platform for the attachment of multiple ligands leading to enhanced avidity with targeted receptors through multivalent binding. In addition, MIONPs have unique magnetic properties, rendering them suitable for

cellular and biological imaging, particularly for MRI. Unlike the toxic heavy metal-containing NPs such as quantum dots, MIONPs have been approved for clinical uses with minimum cytotoxicities [22,23].

Several classes of MNPs with a wide range of magnetic, physical and chemical properties have been molecularly engineered [24]. These include iron oxide ( $\text{Fe}_x\text{O}_y$ ) [25], various types of ferrites ( $\text{MFe}_2\text{O}_4$  where  $\text{M} = \text{Ni}, \text{Co}, \text{Mg}, \text{Zn}, \text{Mn}$ ) [26], metallic colloidal nanocrystals ( $\text{Fe}, \text{Ni}, \text{Co}$ ) [27], and alloys ( $\text{FePt}$ ) [28]. In particular, MIONPs made of ferrites (i.e.  $\text{Fe}_3\text{O}_4/\text{Fe}_2\text{O}_3$ ) were the center of tremendous investigations since the NPs can be easily synthesized from cheap salt materials and can serve as highly efficient contrast agents with high magnetic moments and minimal inherent toxicities. The size of magnetite ( $\text{Fe}_3\text{O}_4$  or  $\text{FeO}\cdot\text{Fe}_2\text{O}_3$ ) or its oxidized form maghemite ( $\gamma\text{-Fe}_2\text{O}_3$ ) NPs ranges from 1 to 100 nm (core diameter). When coated with hydrophilic stabilizers and targeting biomolecules (i.e. antibodies, peptides, proteins, nucleic acids, carbohydrates etc.), the NPs become biologically relevant [29,30]. Nonetheless, the impeccable means to achieve a series of size-controlled, narrowly-dispersed, uniform, highly-magnetic, stable, and biocompatible “all-in-one” MNPs for biomedical and clinical applications remain unambiguously challenging.

### Preparation of MIONPs

Iron (Fe), the fourth most common element in the Earth's crust, exists in a wide range of forms and oxidation states (-2 to +8, the most common being +2 and +3). Due to its four (i.e.  $\text{Fe}$  or  $\text{Fe}^{2+}$ ) or five (i.e.  $\text{Fe}^{3+}$ ) unpaired electrons in the 3d orbital, iron has a strong magnetic moment. When crystals are formed from iron, they can thus be in ferromagnetic, antiferromagnetic or ferrimagnetic states; superparamagnetism is exhibited by small ferromagnetic or ferrimagnetic nanoparticles [4,10,31]. The most common of all are iron oxides and/or oxyhydroxides, which exist in sixteen different forms, are widespread in nature, and play important roles in many environmental and biological processes. MIONPs are mainly made of magnetite or/and maghemite. Magnetite is the most magnetic of all the naturally occurring minerals on Earth [32].

Magnetite NPs having single domains (sizes ~30-70 nm) or pseudo-single domain magnetization states (~70 nm to 20  $\mu\text{m}$ ) are the dominant carriers of remnant magnetization. When the size of the NPs is below a critical value (~20 nm), the individual NP behave like a giant paramagnetic atom with a single magnetic domain, exhibiting superparamagnetic behavior. Superparamagnetic NPs respond rapidly to an applied magnetic field, but exhibit negligible residual magnetism away from the magnetic field, making them especially attractive in advanced biomedicine [33]. The clinical success of using such superparamagnetic NPs (chiefly as liver and lymph nodes contrast imaging probes) made such particles particularly appealing for extensive research [26,34]. Consequently, much research has been devoted to the syntheses of such particles

in ways that examine their sizes, magnetism, stabilization and functionalization.

Particular attention should be directed to the synthetic methods of MIONPs as those can significantly affect the size, shape, structure, dimensions, properties and, hence, the fate of nanocomposites in respective applications. When designing synthetic method, the following central features need to be considered:

- 1) size-controlled and narrowly dispersed (i.e. uniform-size variation <5%) nanocomposites;
- 2) stable and colloidal dispersions;
- 3) large-scaled and reproducible NPs.

Publications describing efficient synthetic routes to prepare shape/size-controlled, highly stable, colloidal, and biocompatible MNPs are immense. Those include non-aqueous and aqueous sol-gel, spray/laser pyrolysis, sonochemical, microemulsion, hydrothermal, and the most popular co-precipitation and thermal decomposition techniques [4,5,7,29]. The major difficulty in designing any synthetic route is to employ simple, practical, and cost-effective ways to produce large quantities of magnetite nanopropbes that are stable for months and don't precipitate from their dispersions. The other key factor is, using the above approach, to get uniform nanocolloids with controlled size and morphology. Of the numerous methodologies developed, two main synthetic solution-based routes have been popularized: a) co-precipitation of iron salts in basic aqueous media stabilized in the presence or absence of surfactants/polymers to produce hydrophilic MNPs [35-38]; b) *high-temperature thermal decomposition* of organometallic precursors ( $\text{Fe}(\text{Cup})_3$ ,  $\text{Fe}(\text{CO})_5$ ,  $\text{Fe}(\text{acac})_3$ , Fe-oleate, Fe-carboxylate or mixed  $\text{M}^{2+} + \text{Fe}^{23+}$ -oleate) in high boiling solvents at elevated temperatures (200-360 °C) to yield hydrophobically-coated MNPs with marked improvements in size control, monodispersity and uniformity [39-46]. Ligand-exchange approaches are then typically employed to replace the hydrophobic chains on the particle surface by hydrophilic biomolecules rendering them dispersed in aqueous media [47-50]. Essentially, these are the two main synthetic methods employed for the preparation of biocompatible MIONPs utilized for medical and biological endpoints. Herein, the above two methods will be discussed in details, along with the pros and cons of each.

### Co-Precipitation method

The co-precipitation procedure is probably the simplest, easiest and fastest methodology to obtain magnetic nanoparticles with a decent control in size, shape and uniformity. Magnetite or its maghemite NPs are prepared by aging appropriate stoichiometric ratios of ferrous ( $\text{Fe}^{2+}$ ) and ferric ( $\text{Fe}^{3+}$ ) salts in an aqueous basic media (typically  $\text{NH}_4\text{OH}$  or  $\text{NaOH}$ ) at room or elevated temperatures (~80-100 °C). This protocol was first explored by Massart in 1981 and is, therefore, known as the “Massart method” [35]. Usually hydrolysis of iron ions (solvated

cations) occurs accompanied with the formation of oxo-ligands. The magnetic NPs, thus, produced are mostly spherical, negatively charged, and relatively homogenous in size and shape. The yield, size, shape, surface properties and polydispersity of the final material depend on many factors including the sequence of addition of reagents, pH, temperature, stirring or mechanical agitation, and nature/concentration of the iron salts.

Changes in any of these parameters determine the composition of the nanocrystal and, consequently, the electrostatic surface charge and density of the NPs. In an excellent report, the effects of these different factors on the quality of the obtained NPs have been discussed [51]. According to the thermodynamics of this reaction, complete precipitation of ferrihydrite/iron oxides in the presence of base (preferably  $\text{NH}_4\text{OH}$ ) should be expected at a pH ( $\sim 10-14$ ), with a stoichiometric ratio of ( $\text{Fe}^{3+}/\text{Fe}^{2+}$ , 2:1). When preparing magnetite, reaction should be done under inert atmosphere to protect against its oxidation to maghemite or hematite ( $\alpha\text{-Fe}_2\text{O}_3$ ).

Although a large amount of NPs can be synthesized using this process, the control of particle size distribution in aqueous media is limited often leading to particle agglomerations (the process by which NPs clump together), since only kinetic factors are controlling the growth of the crystal. A typical precipitation procedure to produce magnetite with relatively good size, shape and uniformity consists of mixing a solution of  $\text{FeCl}_3 \cdot 6\text{H}_2\text{O}$  and  $\text{FeCl}_2 \cdot 4\text{H}_2\text{O}$  (2:1 molar ratio) with mechanic agitation of about 2000 rpm under inert atmosphere. The resulting solution is heated to 70-100 °C, and immediately the speed is elevated to 7500rpm while adding quickly a solution of  $\text{NH}_4\text{OH}$  (10 % by volume). A dark precipitate of  $\text{Fe}_3\text{O}_4$  magnetite NPs will be formed.

In an alkaline medium of pH > 8, polarizing or highly charged cations or anions (i.e. ammonium or alkaline) may give rise to flocculation or agglomeration. Small NPs have an extremely high surface area to volume ratio and cluster easily to minimize their surface energy. Thus, the addition of chelating organic anions (i.e. carboxylates, phosphates, and sulfates) or complexing polymers (e.g. dextran, polyethylene glycol (PEG), polyvinylpyrrolidone (PVP), polyglutamic acid (PGA), polyvinyl alcohol (PVA), polyacrylic acid (PAA), polylactic acid (PLA), poly(lactic-co-glycolic acid) (PLGA) etc. during the formation of iron oxides prevent the agglomeration to certain extent, and imparts protection and stabilization to the NPs [6].

According to the nature of the organic coat, and the molar ratio between the coat and the iron salts, the chelation of these organic ions/complexing polymers on the iron oxide surface can either prevent nucleation and then lead to larger particles or inhibit the growth of the crystal nuclei, leading to small NPs. The coat further protects and stabilizes the magnetic core from the surrounding environments for a long period of time preventing the core material from degradation or oxidation. In addition to stability, the coating renders the NPs biocompatible, which

is significant for biomedical applications. In many cases the protecting coat can be used for further functionalization, i.e. with other NPs or targeting ligands (i.e. carbohydrates, antibodies, cell penetrating peptides, small peptides, aptamers, folic acid) [30]. For instance, dextran-coated iron oxide-based magnetic materials (i.e. CLIONs, SPIONs, USPIOs and related systems) have been clinically approved for imaging of liver lesions and lymph nodes (i.e. Feridex®, Resovist®, Sinerem®) [52, 53]. Full panel of significant studies and investigations including detection, *in-vitro* and *in-vivo* imaging of inflammatory diseases, gene/drug delivery and cellular trafficking have been performed on those particles [54-58].

On the other hand, a silica-coated magnetic material is also extensively utilized and has been used in clinical imaging (GastroMARK®), due to their reactive silanol surface groups [31,59]. A clear advantage of this approach is the easy, versatile and well-established chemistry used for further modification of the surface with the different commercially available siloxanes. Accordingly, any silanol-coated nanoparticle surface can be tailored with different functionality (amines, acids, azides etc.) on demand simply by conjugating the surface hydroxyl groups with the different commercially available alkoxy silanes such as aminopropyltriethoxysilane [60-62]. The physical, chemical, and surface properties of ferumoxides (dextran coated,  $\sim 35$  nm), ferumoxtran (dextran covered,  $\sim 21$  nm), and ferumoxsil (siloxane coated,  $\sim 300$  nm) prepared *via* the co-precipitation methods have been reported [63,64].

### Thermolysis Method

Marked improvements in size control, uniformity and monodispersity have been achieved using organic-based thermolysis procedures. The synthesis of such nanocrystals have popularized two major synthetic methods: "hot-injection" by rapid introduction of reagents into the hot solution ( $\geq 300$  °C) containing surfactants or "heating-up" a pre-mixed solution of precursors, surfactants, and solvent to a certain temperature to achieve the burst of nucleation and initiate the particle growth [65]. The hot-injection method was devised to induce a very high level of supersaturation at the start of the synthetic reaction. Upon injection, the extremely fast reaction of the precursor directly leads to a sudden increase in the supersaturation level in the solution and, hence, the formation of nanocrystals starts immediately [66]. On the other hand, in the heat-up synthesis, the reaction mixture is prepared at a lower temperature and heated to temperatures (up to 360 °C).

This simple procedure has been successfully utilized to synthesize monodisperse nanocrystals of a wide range of materials [67]. High temperature reduction of metal salts in the presence of stabilizing agents is one of the most noteworthy heat up techniques used to produce monodisperse nanocrystals of many metals and metal oxides, including magnetic ferrites. Among the many examples, thermal decomposition of organometallic compounds (i.e. iron-oleate complex) in high-

boiling-point nonpolar organic solvents (i.e. benzyl ether) has proven to be an attractive route for the synthesis of highly monodisperse, uniform and crystalline nanocrystals. Hyeon et al. synthesized superparamagnetic maghemite  $\gamma\text{-Fe}_2\text{O}_3$  nanocrystals *via* a high-temperature aging of iron-oleic metal complex using iron pentacarbonyl ( $\text{Fe}(\text{CO})_5$ ) in the presence of oleic acid in dioctyl ether at 100 °C and heating up to 300 °C to produce uniform iron nanoparticles [41].

In 2004, instead of using the toxic and expensive  $\text{Fe}(\text{CO})_5$ , the same group reported the elegant ultra-large-scale synthesis of monodispersed nanocrystals via the slow heating of metal-oleate complex and oleic acid in high boiling solvents [39]. Cheon et al. [68] prepared well-defined single-crystalline  $\gamma\text{-Fe}_2\text{O}_3$  nanocrystals with different shapes ranging from diamonds, triangles to spheres were also synthesized using the thermolysis of  $\text{Fe}(\text{CO})_5$  in the presence of various capping ligands (i.e. dodecylamine). Various metal NPs were also synthesized using the heat-up thermal decomposition method. Sun and his colleagues prepared highly uniform monodisperse FePt nanoparticles by heating a reaction mixture containing platinum acetylacetonate,  $\text{Fe}(\text{CO})_5$ , 1,2-hexadecanediol, oleic acid and oleyl amine [44].

Based on this method, the Sun group enclosed the most cited and widely followed synthesis of highly monodispersed controlled-sized magnetite  $\text{Fe}_3\text{O}_4$  nanoparticles (4 nm) from a high-temperature (200 – 300 °C) 1,2-hexadecanediol solution of iron(III) acetylacetonate ( $\text{Fe}(\text{acac})_3$ ) in the presence of oleic acid and oleylamine [43]. Larger size nanoparticles (8,12,16nm) can be formed *via* seed-mediated growth of the smaller nanocrystals. By controlling the quantity of nanoparticle seeds, different sizes of nanoparticles can be synthesized. Furthermore, different sizes of metal ferrites ( $\text{MFe}_2\text{O}_4$ , where  $\text{M}=\text{Co}$ ,  $\text{Fe}$ ,  $\text{Mn}$ , etc.) were also prepared in the form of monodisperse nanoparticles by the seed-mediated growth process using  $\text{Fe}(\text{acac})_3$  and  $\text{M}(\text{acac})_2$  as reactants [46].

In another noteworthy report, Jana et al. reported the synthesis of size- and shape-controlled magnetic ( $\text{Fe}$ ,  $\text{Cr}$ ,  $\text{Mn}$ ,  $\text{Co}$  and  $\text{Ni}$ ) oxide nanocrystals based on high-temperature pyrolysis of metal fatty acid salts as the precursors and alkylamines as the activation reagents in noncoordinating solvents (octadecene) heated at 300°C under inert atmosphere [69]. Mechanistically, an important factor when preparing uniform monodisperse NPs in the solution phase is to separate nucleation and growth steps. During the synthesis, two stages are involved:

- 1) short burst of nucleation where the monomers quickly reach critical supersaturation without further formation of nuclei afterwards;
- 2) slow growth of the produced nuclei at the same rate by diffusion of the solutes to the surface of the crystal [70,71]. Ideally, the two stages should be separated and nucleation

should be avoided during the period of growth.

The basic concepts to control the size distribution and the nanocrystal formation mechanism are, thus, largely based on the classical LaMer model [72], namely, burst of nucleation, diffusion-controlled growth, and Ostwald ripening (redeposition of small crystals onto larger ones). Typically, control over monodispersity must be performed during the very short nucleation period. If the percentage of the nanoparticle growth during that period is small compared with subsequent growth, the particles can become more uniform over time. Studies and observations have shown that enhanced uniformity with better size distributions can occur at high temperatures in organic solvents and is more difficult to form in an aqueous media at room temperature. For mechanistic insights and more theoretical explanations on the formation of such monodisperse and uniform nanocrystals, including metals and their oxides, readers are referred to the following excellent reviews [65,67].

Despite the thorough investigations and success of the high-temperature organic thermolysis, these methods have problems and limitations. First, it is necessary to heat the reaction mixture to very high temperatures up to 360 °C which needs highly trained personnel and, in practice, is dangerous and tedious. Second, the polyalcohol components used as the iron reducing agent are not only expensive, but also cause many side reactions of polyaldehydes and polyorganic acids making the process of separating the byproducts complicated. Besides, complex and difficult multi-step processes of synthesizing and purifying the intermediate precursors are applied reducing the reaction efficiencies [73].

All this often leads to inconveniency for industrial scale-up. Finally, there is a limit to the choice of the NP capping agents which should be only long hydrophobic alkyl chains. This is a chief and major disadvantage of the thermolysis approaches, as no polymers can be directly used and the final product is, thus, only dispersible in organic nonpolar solvents (i.e. hexanes). The resulting insolubility in water greatly limits their biological applications.

Consequently, a reasonable approach is to tune the solubility of these high-quality organic-dispersed NPs and transfer them into aqueous media to be conjugated with various water-soluble biomolecules. A “ligand-exchange” strategy, where the hydrophobic chains on the particle surface are replaced by molecules containing polar groups, is typically employed [47,48,74]. We [49] and others [50] successfully demonstrated the exchange of hydrophobic acids from the surface of MIONPs to make water-dispersible particles. Cheon group exchanged the hydrophobic lauric acid capping ligands with 2,3-dimercaptosuccinic acid (DMSA) to render them water-soluble [45]. In the above example, the polyelectrolyte ligand forms a stable coating through its carboxylic chelate bonding to the nanocrystal particle surface. The remaining free thiol

groups in DMSA allowed the attachment of target-specific cancer-targeting antibodies (i.e. Herceptin). Cap exchange with bifunctional ligands has also found wide use, since the remaining functional groups will be available for further coupling to bioactive targeting molecules of interest.

Examples to improve on the thermal decomposition in organic solvents with diverse morphologies and shapes obtained [69,75] or to fabricate one-step water-soluble monodisperse magnetite NPs have been reported. For instance, Li and coworkers reported one-pot thermal decomposition of  $\text{Fe}(\text{acac})_3$  using strong polar 2-pyrrolidone as a coordinating solvent to produce water-soluble magnetite nanocrystals [76]. They also have succeeded in preparing water-soluble magnetite nanocrystals simply by refluxing inexpensive hydrated ferric salts in 2-pyrrolidone [77]. Ge et al. [78,79] synthesized water-soluble magnetite nanocrystals by rapidly injecting a preheated  $\text{NaOH}$ /diethylene glycol solution into a mixture of  $\text{PAA}/\text{FeCl}_3$ /diethylene glycol heated at  $\sim 245^\circ\text{C}$ . Nevertheless, these methods are used to much lesser extent by researchers.

### Ko-precipitation Hydrolytic Basic (KHB) method

In our recent work, we sought to design a method of producing well-controlled narrowly dispersed magnetic metal oxide nanocolloids [80]. The approach relies on sequential basic hydrolytic *in situ* precipitation (*Ko-precipitation*) of inexpensive and nontoxic metal salts compartmentalized by stabilizing organic acids (hydrophobic acids, polymeric acids, amino acids or polyamino acids) and amines, without the use of high-boiling

point solvents and elevated temperatures (up to  $360^\circ\text{C}$ ). The so-called "*Ko-precipitation Hydrolytic Basic (KHB)*" method consists of the following components: inexpensive metallic ions dissolved in aqueous media (i.e.  $\text{Fe}^{3+}$  and  $\text{M}^{2+}$  salts, where  $\text{M} = \text{Sc}, \text{Ti}, \text{V}, \text{Cr}, \text{Mn}, \text{Fe}, \text{Co}, \text{Ni}, \text{Cu}$  and  $\text{Zn}$ ), organic carboxylic acid surfactants including saturated or unsaturated hydrophobic acids ( $\text{C}_n\text{COOH}$ ,  $\text{C}_n$ : hydrocarbon,  $6 < n < 30$ ) or polymeric acids (i.e. hyaluronic acid (HA), carboxymethyl dextran and their acid-based derivatives, acrylic-based polymers PAA, PLA, PLGA, or amino acids (i.e. arginine, lysine, glutamic acid) and their polyamino acids, in addition to co-surfactants (alkylamines  $\text{C}_n\text{NH}_2$ ,  $\text{C}_n$ : hydrocarbon,  $6 < n < 30$ ), and a base ( $\text{NH}_4\text{OH}$  or  $\text{NaOH}$ ).

In a specific example, iron oxide nanocolloids were prepared by sequentially mixing  $\text{Fe}(\text{III})$  salts, with different concentrations of the acid (1.5–15 mmol), to advantage oleic acid, for 20 minutes. Subsequently, the hydrophobic amine (1–15 mmol), to advantage hexylamine, was added into the mixture and stirred vigorously under an inert atmosphere. To the above mixture, aqueous solution of  $\text{Fe}^{2+}$  salt, to advantage  $\text{FeCl}_2$ , was added in a molar ratio  $\text{Fe}(\text{III})/\text{Fe}(\text{II}) = 2$ . Addition of the base ( $\text{NH}_4\text{OH}$ ) allowed the formation of ultra-small, ultra-stable, and well-dispersed nanocolloids of iron oxides. The particle size can be tuned from 2 to 6 nm by controlling the acid to iron precursor molar ratios (Figure 1). The obtained nanocrystals are isolated and purified by simple centrifugation without size-selective purifications and are readily redispersed in various solvents (depending on the hydrophilicity of the functionalized acid) for months with remarkable stabilities.

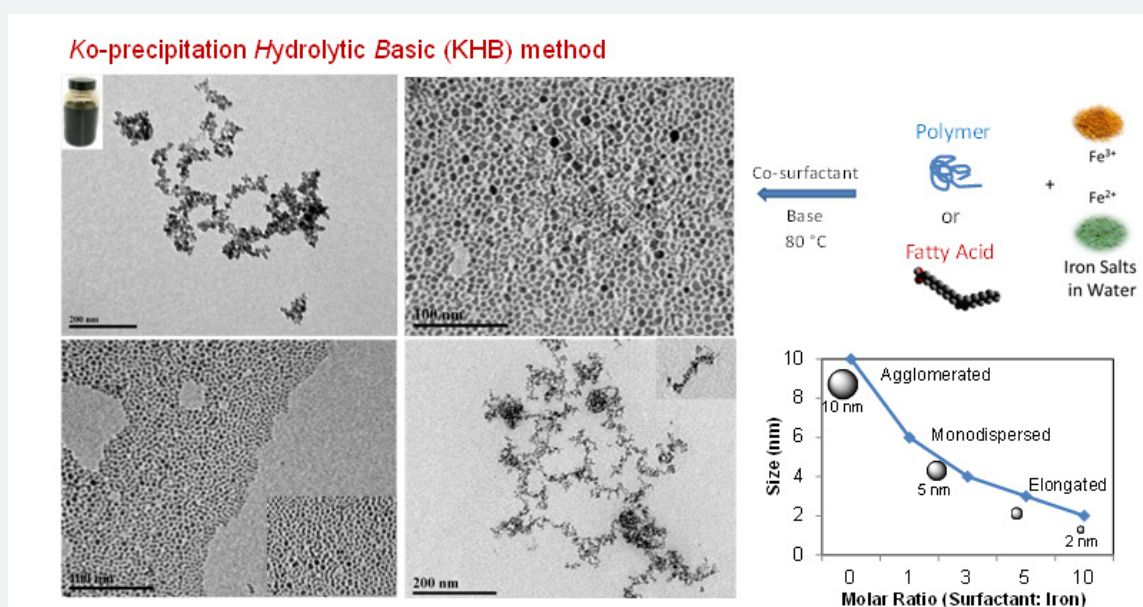


**Figure 1:** Schematic representation for the synthesis of ultra-small, ultra-stable, and well-dispersed magnetic iron oxide nanocolloids. The NP sizes can be tuned from 2 to 6 nm by controlling the acid to iron precursor molar ratios [80].

In summary, the thermal decomposition techniques allow for high control over size, shape and size distribution, but low control over water-soluble, biocompatible, highly-magnetized and ready-to-use MNPs. These high-temperature thermolysis methods are complicated, costly, relatively toxic, and industrially-limited. On the other hand, synthesizing metal oxide nanoparticles by aqueous basic co-precipitation of metallic salts in water, whether with or without coatings, often lead to relatively agglomerated MIONPs with some difficulties in achieving narrow size distributions. Our KHB methodology, thus, offers the simplicity of the conventional iron salt co-precipitation, with the high-quality and narrowly dispersed capability usually obtained by the thermolysis processes. This methodology, thus, offers simpler, faster, non-tedious, and tailor-made strategy to effectively produce various acid-stabilized controlled, colloidal and stable monodisperse MNPs dispersed in hydrophilic or hydrophobic solvents, on demand.

### Utilization of MNPs for cancer therapy and multimodal imaging

Directing the delivery and enhancing the efficacy of drugs using functional MNPs will help carry pharmaceutical chemotherapeutic drug and significantly enhance its local concentration in the damaged area making the nano-therapeutic approach extremely beneficial. The clinical significance of drug delivery systems lies in the ability to specifically direct a drug or drug carrier to intended targets to minimize conventional drug-originated systemic toxic side effects.

In general, drug delivery to the target can be achieved by either passive targeting because of the so called enhanced

permeability and retention (EPR) effect of leaky tumor vasculature or active targeting directed to cell-surface receptors (ligand-receptor interactions), antigens (antibody antigen binding), or carbohydrates (lectin-glycoconjugate interactions) [81]. For effective delivery, the MNP system should: 1) possess large payloads of drugs per NP attached and delivered; 2) be targeted to a specific molecular target, and 3) allow controlled release of drugs at the intended target intracellularly and intratumorally with high efficiencies. A wide variety of drugs can be loaded onto MNPs by chemical or physical functionalization for drug delivery applications. The conjugated drugs then have to be administrated, and then successfully released. There are two main routes for drug release: a) locally-activated or b) externally-activated. The former can take place by simple diffusion and/or through different endocytic mechanisms requiring chemical and biochemical stimuli (i.e. pH, hydrolysis, enzymatic activities etc.) triggering the drug release.

Typically, NPs, depending on their sizes and surface charges, chose either endocytic, phagocytic, pinocytic, or receptor-mediated pathways for cellular internalization [82]. Externally-activated targeting, on the other hand, is based on external factors, such as external magnetic field (i.e. magnetic drug targeting), light, temperature, and ultrasound [83]. Such stimuli-responsive NPs have demonstrated, though to varying degrees, improved *in-vitro* and/or *in-vivo* drug release profiles. In addition, dual and multi-stimuli responsive NPs that respond to a combination of two or more signals with precision site-specific drug delivery have been lately examined [84].

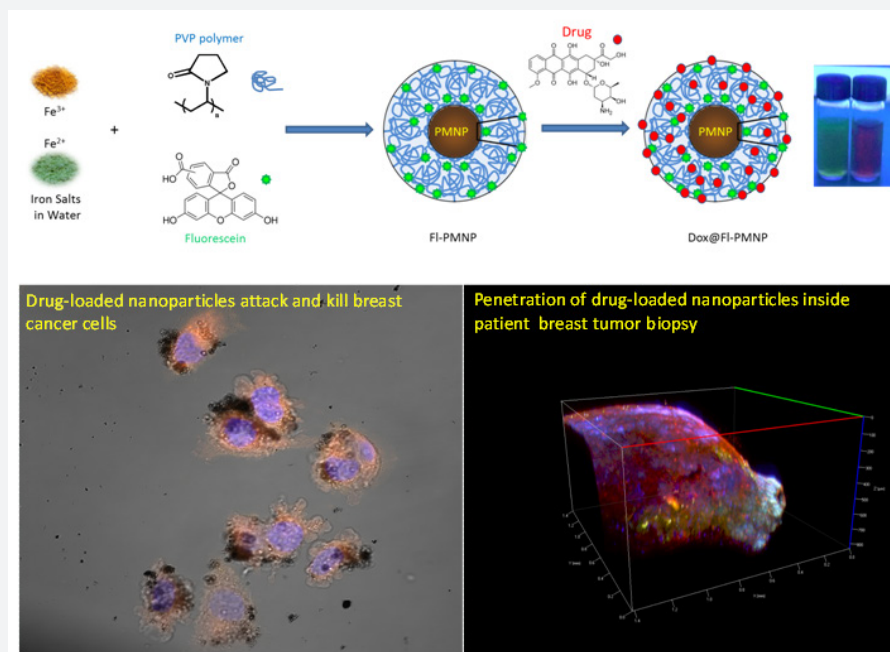


**Figure 2:** Schematic illustration for the preparation of colloidal drug-conjugated MNPs via sequential Ko-precipitation basic hydrolysis of iron salts in the presence of fluorescein (FI) and PVP complexing polymer. The drug-loaded NPs attack metastatic breast cancer cells, causing apoptotic cell death, as well as penetrated patient solid tumor biopsies (~ 150 μm deep into the tumor) delivering the anticancer drug intratumorally

Recently, our group developed a chemotherapeutic nanoformulation made of PVP-stabilized magneto-fluorescent nanoparticles (Fl-PMNPs) loaded with Dox (Figure 2) and studied its delivery towards human breast cancer cells, 3D primary tumors, and solid tumors [85]. When tested *in vitro*, Dox@Fl-PMNPs were found to be more effective in killing the metastatic breast cancer cells (2 to 3 fold enhanced cytotoxicities for MDA-MB-231 compared to MCF-7), with considerably less toxicity towards the normal non-tumorigenic breast cells MCF-10A, suggesting huge potentials as selective anti-cancer agents for breast cancer therapy. Importantly, Dox@Fl-PMNPs were also able to effectively penetrate and deliver drugs to 3D forming primary tumor cells and patient tumor biopsies. These results open new opportunities for potential important clinical improvement of chemotherapy to tumors. This delivery vehicle was based on passively targeting the anticancer drug without a specific-receptor targeting approach.

When active targeting is sought, specific targeting ligands have to be conjugated to the NP surfaces. The conjugation are typically based on two main chemistries:

- 1) reactive functionalities present on the nanomaterial platforms;
- 2) functional groups present on the targeting ligands (proteins, peptides, carbohydrates, antibodies, nucleic acids, folic acid, enzymes, genes, growth factors, imaging agents etc.) to be conjugated [30].

The target biomolecules can be specifically labeled with fluorescent probes, dyes, tags, crosslinking reagents or imaging agents before being attached to the NP surface. The functionality of the NP surface can be also tailored to attach certain probes. Many bio-conjugation strategies are typically used to functionalize the surface of NPs with the various targeting ligands or/and imaging agents via covalent, noncovalent, encapsulation, electrostatic or hydrophobic-hydrophobic conjugations [86].

Particularly interesting is the immobilization of imaging or fluorescent probes on MNPs which has recently attracted much attention since it is a powerful means for mediating the use of targeted functional nanomaterials in biomolecular imaging [87]. Fluorochromes coupled to the nanoparticulate allow optical imaging including fluorescence reflectance imaging, fluorescence mediated tomography (FMT), confocal microscopy, flow cytometry, and near-infrared (NIR) fluorescence-imaging. In particular, fluorochromes that emit in the NIR spectral window (preferably VT680, AF680 or Cy5.5) penetrate tissue for several centimeters, thereby rendering fluorescence imaging techniques possible. Moreover, molecular imaging with high-relaxivity contrast MRI probes is one of the most promising diagnostic approaches in biomedicine offering resolution of anatomy and detection of associated disease biomarkers [33,57]. The development of MIONP contrast agents for use in multimodality diagnostic imaging has also been proposed [87,88]. MRI, X-ray computed tomography (CT), positron emission tomography

(PET) and fluorescence imaging display complementary strengths in terms of spatial and temporal resolution, the possibility to generate contrast, sensitivity, and multiplex imaging [89]. An appealing construct in probe development is, thus, to design all-in-one targeting agents that can be detected with multiple techniques. Therefore, multimodal labeled MIONP agents have been pursued for such purposes.

Josephson et al. conjugated arginyl peptides to CLIO, followed by the attachment of the indocyanine dye Cy5.5, allowing lymph nodes detection by MRI and NIR fluorescence simultaneously [90]. Moore et al. prepared cancer targeted multimodal imaging probes consisting of Cy5.5-CLIO attached to FITC-labeled EPPT peptides *via* thioether linkage to target the underglycosylated mucin-1 (uMUC-1) antigen *in-vitro* and *in-vivo* [91]. In an elegant report, Pittet et al. described the preparation of magnetofluorescent nanoparticles for immune T-cell labeling *in-vitro* and multimodal imaging of administered cells *in-vivo* [92]. In their work, amine reactive NHS-ester fluorochromes were attached to CLIO-NH<sub>2</sub>, and then reacted with either FITC-labeled HIV-Tat peptide or protamine *via* the bifunctional succinimidyl iodoacetic acid or amide coupling, respectively, to yield fluorescent magnetic nanoprobe having membrane-translocating properties.

In another study, Nahrendorf et al. [93,94] have exemplified the usefulness of trimodal imaging probes where they labeled a dextranated and DTPA-modified magneto fluorescent nanoparticle (20 nm) with the PET tracer <sup>64</sup>Cu to yield a PET, MRI, and optically detectable probe allowing imaging of macrophages in inflammatory atherosclerotic plaques. Following this study, the same group embarked on the synthesis of hybrid PET-CT/FMT optical imaging probes (<sup>18</sup>F-CLIO-VT680) containing the clinical PET <sup>18</sup>F isotope and a far red fluorochrome (VT680) for FMT, fluorescence histology and flow cytometry (Figure 3a). The aminated CLIO were reacted with hydroxysuccinimide-derivatized fluorochromes and azides for clicking short <sup>18</sup>F-PEGs to their surfaces. Importantly, the NPs can be further reacted with targeting ligands or other chelators depending on the intended target. Using a mouse model of cancer and their different imaging constructs, they demonstrated the distinct tumoral locations in multiple channels *in-vivo* by measuring tumoral proteases, macrophage content and integrin expression simultaneously.

The combined FMT/PET-CT multichannel imaging offers parallel interrogation of up to five molecular targets. This capability enhances the simultaneous examination of biomarker clusters, and will ultimately improve our understanding of the underlying biological mechanisms. In another report, the Cheon group fabricated all-in-one Mn-doped magnetism-engineered iron oxide nanoparticles (Mn-MEIONPs) for simultaneous molecular imaging and targeted siRNA delivery *in-vitro* [95]. MnMEIO-siGFP-Cy5/PEG-RGD nanoparticles were prepared by treating a BSA coated-MnMEIO with the bifunctional

N-succinimidyl-3-(2-pyridyldithio)propionate (SPDP) and subsequent reaction of the SPDP-activated nanoparticles with the thiolated siRNA-Cy5 or PEG-RGD through disulfide

bonds (Figure 3b). Not only fluorochromes were conjugated to the surface of MIONPs, but also gadolinium ion ( $Gd^{3+}$ ) based multimodal imaging probes were also developed.

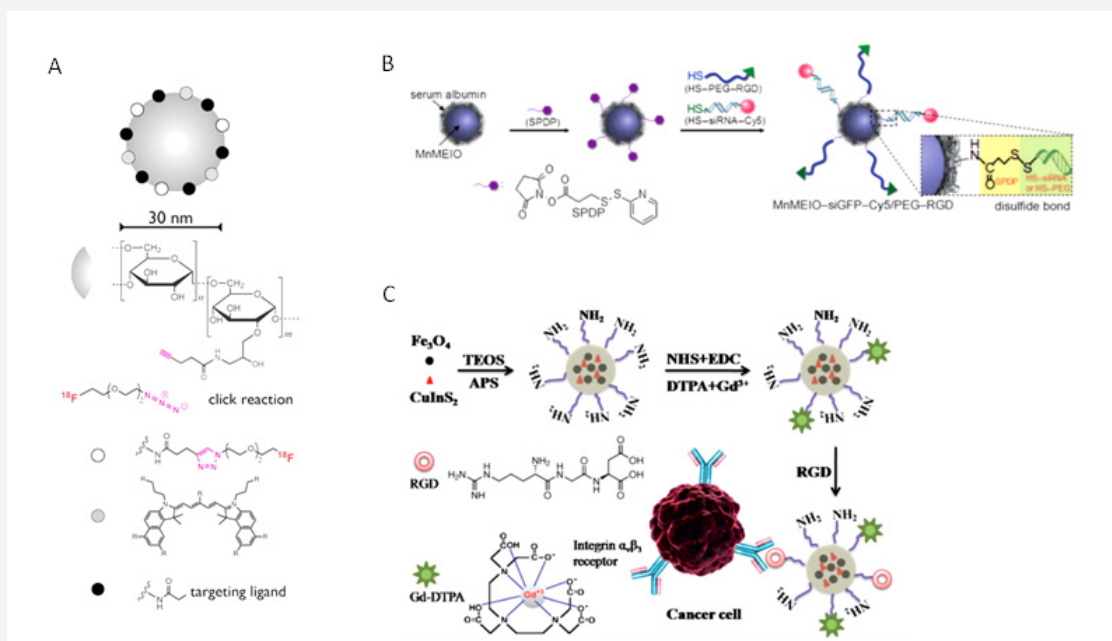


**Figure 3:** Different imaging agents ( $^{18}F$ -PET, fluorescent, Gadolinium) conjugated to the surface of MNPs. A) 30 nm dextran-coated MNP attached to clinical PET isotope  $^{18}F$  via click chemistry and a near-infrared fluorochrome for FMT. [94]. B) Schematic illustration for the synthesis of multimodal MnMEIO-siGFP-Cy5/PEG-RGD. [95]. C) Synthetic scheme for the formation of  $Fe_3O_4/CIS@SiO_2(Gd-DTPA)$ -RGD NPs composed of multifunctional Gd-labeled  $Fe_3O_4$  NPs and CuInS<sub>2</sub> (CIS) quantum dots for targeted tri-modal T1-, T2-weighted MR and fluorescence imaging. [85]

Various Gd(III) complexes and Gd conjugates to different inorganic, biological or polymeric platforms have been developed in an effort to enhance MR bright imaging of targeted organs and tissues as a tool for clinical diagnostics [96]. Several reports have shown that Gd-bound nanoformulations (targeted and non-targeted) offer several times higher T1 relaxivities, and hence brighter contrast, than those corresponding to nonbound Gd chelates. Bae et al. [97] synthesized gadolinium-labeled biocompatible magnetite NPs (GMNPs) and demonstrated their use as dual contrast agents for T1- and T2-weighted MRI images by conducting *in-vitro* and *in-vivo* imaging. Oleic acid-coated magnetite nanoparticles were surface-exchanged with a mixed layer of 3,4-dihydroxy-L-phenylalanine (DOPA)-conjugated PEG and dopamine *via* strong coordination bonds of their catechol groups with the surface of iron oxides [98]. While PEG renders the particles water dispersible, the amine-terminated dopamine allows subsequent modification with Gd-DTPA through the formation of an isothiourea bond with an isothiocyanate bond of DTPA.

Shen et al recently prepared Gd-labeled superparamagnetic  $Fe_3O_4$  NPs and fluorescent CuInS<sub>2</sub> (CIS) quantum dots conjugated with RGD peptides (Figure 3c) for tri-mode targeted T1-, T2-weighted magnetic resonance and fluorescence imaging of pancreatic cancer [99]. The T1-weighted positive and T2-

weighted negative enhancement in MRI significantly improves the diagnosis accuracy, and fluorescence imaging of tumor tissue can assist in clinical surgery. All these examples suggest potential use of functionalized multifunctional MNPs as a promising platform for multimodal imaging.

## Conclusion

MNPs hold great promise for biomedical theranostic applications particularly as imaging agents and drug delivery carriers. Such potential stems from their unique intrinsic physiochemical and biochemical properties including excellent magneto-responsive properties, low toxicity, colloidal stability, and facile surface engineering capability. The main advantages of using MNPs are: 1) easy preparation; 2) small size; 3) facile surface functionalization; 3) excellent biocompatibility and stability; 4) efficient drug conjugation; and 5) superior magnetic responsiveness. Such unique properties enabled their use as MRI contrast agents, hyperthermia agents, magnetic field guided localization vectors, and/or drug delivery vehicles. Moreover, they can be used for image guidance during drug delivery processes and non-invasive imaging to enhance delivery and/or combined therapeutic effect. MNPs are excellent candidates for targeted drug delivery and image-guided therapeutics with a great promising potential in clinical theranostics.



## Acknowledgments

This work is supported by KAIMRC through grant RC13/204/R. The author acknowledges the continuous support by KSAU-HS and NGHA

## References

- Mann S (2009) Self-assembly and transformation of hybrid nano-objects and nanostructures under equilibrium and non-equilibrium conditions. *Nat Mater* 8(10): 781-792.
- Schroeder A, Heller DA, Winslow MM, Dahlman JE, Pratt GW, et al. (2011) Treating metastatic cancer with nanotechnology. *Nat Rev Cancer* 12(1): 39-50.
- Fan H, Yang K, Boye DM, Sigmon T, Malloy KJ, et al. (2004) Self-assembly of ordered, robust, three-dimensional gold nanocrystal/silica arrays. *Science* 304(5670): 567-571.
- Lu AH1, Salabas EL, Schüth F (2007) Magnetic nanoparticles: synthesis, protection, functionalization, and application. *Angew Chem Int Ed* 46(8):1222-1244.
- Laurent S, Forge D, Port M, Roch A, Robic C, et al. (2008) Magnetic Iron Oxide Nanoparticles: Synthesis, Stabilization, Vectorization, Physicochemical Characterizations, and Biological Applications. *Chem Rev* 108(6): 2064-2110.
- Gupta AK, Gupta M (2005) Synthesis and surface engineering of iron oxide nanoparticles for biomedical applications. *Biomaterials* 26(18): 3995-4021.
- Ling D, Lee N, Hyeon T (2015) Chemical Synthesis and Assembly of Uniformly Sized Iron Oxide Nanoparticles for Medical Applications. *Acc Chem Res* 48(5): 1276-1285.
- Estelrich J, Escribano E, Queralto J, Busquets MA (2015) Iron Oxide Nanoparticles for Magnetically-Guided and Magnetically-Responsive Drug Delivery. *Int J Mol Sci* 16(4): 8070-8101.
- Laurent S, Saei AA, Behzadi S, Panahifar A, Mahmoudi M (2014) Superparamagnetic iron oxide nanoparticles for delivery of therapeutic agents: opportunities and challenges. *Expert Opin Drug Deliv* 11(9): 1449-1470.
- Wei Wu, Chang ZJ, Vellaisamy ALR (2016) Designed synthesis and surface engineering strategies of magnetic iron oxide nanoparticles for biomedical applications. *Nanoscale* 8: 19421-19474.
- Sun C, Lee JS, Zhang M (2008) Magnetic nanoparticles in MR imaging and drug delivery. *Adv Drug Deliv Rev* 60(11):1252-1265.
- Corot C, Robert P, Idée JM, Port M (2006) Recent advances in iron oxide nanocrystal technology for medical imaging. *Adv Drug Delivery Rev* 58(14): 1471-1504.
- El-Boubbou K, Gruden C, Huang X (2007) Magnetic Glyco-nanoparticles: A Unique Tool for Rapid Pathogen Detection, Decontamination, and Strain Differentiation. *J Am Chem Soc* 129(44): 13392-13393.
- El-Boubbou K, Zhu DC, Vasileiou C, Borhan B, Prosperi D, et al. (2011) Magnetic glyco-nanoparticles: A tool to detect, differentiate, and unlock the glyco-codes of cancer via magnetic resonance imaging. *J Am Chem Soc* 132(12): 4490-4499.
- Wang D, Fei B, Halig LV, Qin X, Hu Z, et al. (2014) Targeted Iron-Oxide Nanoparticle for Photodynamic Therapy and Imaging of Head and Neck Cancer. *ACS Nano* 8(7): 6620-6632.
- Erwin P, Fenghe W, Jun MX (2015) Nanostructured magnetic nanocomposites as MRI contrast agents. *J Mater Chem B* 3: 2241-2276.
- Dakdouki E-MH, Boubbou El-K, Kamat M, Huang R, Abela GS, et al. (2014) CD44 Targeting Magnetic Glyconanoparticles for Atherosclerotic Plaque Imaging. *Pharm Res* 31(6): 1426-1437.
- Kim J, Kim HS, Lee N, Kim T, Kim H, et al (2008) Multifunctional uniform nanoparticles composed of a magnetite nanocrystal core and a mesoporous silica shell for magnetic resonance and fluorescence imaging and for drug delivery. *Angew Chem, Int Ed* 47(44): 8438-8441.
- Kim DH, Guo Y, Zhang Z, Procissi D, Nicolai J, et al. (2014) Temperature Sensitive Magnetic Drug Carriers for Concurrent Gemcitabine Chemohyperthermia. *Adv Healthcare Mater* 3(5): 714-724.
- Jeonghun Lee, Hyunjung Kim, Seahee Kim, Hyemi Lee, Jin Kim, et al. (2011) A multifunctional mesoporous nanocontainer with an iron oxide core and a cyclodextrin gatekeeper for an efficient theranostic platform. *J Mater Chem* 22: 14061-14067.
- Arruebo M, Fernández P- R, Ibarra MR, Santamaría J (2007) Magnetic nanoparticle drug delivery systems for targeting tumor. *Nano Today* 2: 22-32.
- Jain TK, Reddy MK, Morales MA, Leslie P-DL, Labhsetwar V (2008) Biodistribution, Clearance, and Biocompatibility of Iron Oxide Magnetic Nanoparticles in Rats. *Mol Pharmaceutics* 5(2): 316-327.
- Mahmoudi M, Hofmann H, Rothen R-B, Petri F-A (2012) Assessing the in vitro and in vivo toxicity of superparamagnetic iron oxide nanoparticles. *Chem Rev* 112(4): 2323-2338.
- U Jeong, Teng X, Wang Y, Yang H, Xia Y (2007) Superparamagnetic colloids: Controlled synthesis and niche applications. *Adv Mater* 19: 33-60.
- Cheng FY, Su CH, Yang YS, Yeh CS, Tsai CY, et al. (2005) Characterization of aqueous dispersions of Fe<sub>3</sub>O<sub>4</sub> nanoparticles and their biomedical applications. *Biomaterials* 26 (7): 729-738.
- Jun YW, Lee JH, Cheon J (2008) Chemical design of nanoparticle probes for high-performance magnetic resonance imaging. *Angew Chem, Int Ed* 47(28): 5122-5135.
- Puntes VF, Krishnan KM, Alivisatos AP (2001) Colloidal nanocrystal shape and size control: The case of cobalt. *Science* 291(5511): 2115-2117.
- Sun S, Murray CB, Weller D, Folks L, Moser A (2000) Monodisperse FePt nanoparticles and ferromagnetic FePt nanocrystal superlattices. *Science* 287(5460): 1989-1992.
- Sperling RA, Parak WJ (2010) Surface modification, functionalization and bioconjugation of colloidal inorganic nanoparticles. *Philos Trans R Soc* 368(1915): 1333-1383.
- Cortajarena AL, Ortega D, Ocampo SM, Pierre Couleaud, Rodolfo Miranda, et al. (2014) Engineering iron oxide nanoparticles for clinical settings. *Nanobiomedicine* 1: 58841.
- Wang YX, Hussain SM, Krestin GP (2001) Superparamagnetic iron oxide contrast agents: physicochemical characteristics and applications in MR imaging. *Eur Radiol* 11(11): 2319-2331.
- Harrison RJ, Dunin-Borkowski RE, Putnis A (2002) Direct imaging of nanoscale magnetic interactions in minerals. *Proc Natl Acad Sci* 99(26): 16556-16561.
- Thorek DL, Chen AK, Czupryna J, Tsourkas A (2006) Superparamagnetic iron oxide nanoparticle probes for molecular imaging. *Ann Biomed Eng* 34(1): 23-38.
- Prijic S, Sersa G (2011) Magnetic nanoparticles as targeted delivery systems in oncology. *Radiol Oncol* 45(1): 1-16.
- R. Massart (1981) Preparation of aqueous magnetic liquids in alkaline and acidic media. *IEEE Trans Magn* 17(2): 1247-1248.
- Cheng FY, Su CH, Yang YS, Yeh CS, Tsai CY, et al. (2005) Characterization of aqueous dispersions of Fe<sub>3</sub>O<sub>4</sub> nanoparticles and their biomedical

- applications. *Biomaterials* 26(7): 729-738.
37. Kamat M, Boubbou El-K, Zhu DC, Lansdell T, Lu X, et al. (2010) Hyaluronic acid immobilized magnetic nanoparticles for active targeting and imaging of macrophages. *Bioconjugate Chem* 21(11): 2128-2135.
  38. Jing J, Zhang Y, Liang J, Zhang Q, Bryant E, et al. (2012) One-step reverse precipitation synthesis of water-dispersible superparamagnetic magnetite nanoparticles. *J Nanopart Res* 14:827-888.
  39. Park J, An K, Hwang Y, Park JG, Noh HJ, et al. (2004) Ultra-large-scale syntheses of monodisperse nanocrystals. *Nat Mater* 3(12): 891-895.
  40. Park J, Lee E, Hwang NM, Kang M, Kim SC, et al. (2005) One-nanometer-scale size-controlled synthesis of monodisperse magnetic Iron oxide nanoparticles. *Angew Chem, Int Ed* 44(19): 2872-2877.
  41. Hyeon T, Lee SS, Park J, Chung Y, Na HB (2001) Synthesis of Highly Crystalline and Monodisperse Maghemite Nanocrystallites without a Size-Selection Process. *J Am Chem Soc* 123(51): 12798-12801.
  42. Kim BH, Lee N, Kim H, An K, Park Y, et al. (2011) Large-Scale Synthesis of Uniform and Extremely Small-Sized Iron Oxide Nanoparticles for High-Resolution T1 Magnetic Resonance Imaging Contrast Agents. *J Am Chem Soc* 133(32): 12624-12631.
  43. Sun S, Zeng H (2002) Size-Controlled Synthesis of Magnetite Nanoparticles. *J Am Chem Soc* 124(28): 8204-8205.
  44. Sun S, Murray CB, Weller D, Folks L, Moser A (2000) Monodisperse FePt nanoparticles and ferromagnetic FePt nanocrystal superlattices. *Science* 287(5460): 1989-1992.
  45. Jun YW, Huh YM, Choi JS, Lee JH, Song HT, et al. (2005) Nanoscale Size Effect of Magnetic Nanocrystals and Their Utilization for Cancer Diagnosis via Magnetic Resonance Imaging. *J Am Chem Soc* 127(16): 5732-5733.
  46. Sun S, Zeng H, Robinson DB, Raoux S, Rice PM, et al. (2004) Monodisperse MFe<sub>2</sub>O<sub>4</sub> (M = Fe, Co, Mn) Nanoparticles. *J Am Chem Soc* 126(1): 273-279.
  47. Dong A, Ye X, Chen J, Kang Y, Gordon T, et al. (2011) A Generalized Ligand-Exchange Strategy Enabling Sequential Surface Functionalization of Colloidal Nanocrystals. *J Am Chem Soc* 133(4): 998-1006.
  48. Zhang T, Ge J, Hu Y, Yin Y (2007) A general approach for transferring hydrophobic nanocrystals into water. *Nano Lett* 7(10): 3203-3207.
  49. Dakdouki El-MH, E-Boubbou K, Zhu DC, Huang X (2011) A simple method for the synthesis of hyaluronic acid coated magnetic nanoparticles for the highly efficient cell labelling and in vivo imaging. *RSC Adv* 1(8): 1449-1452.
  50. Randy DP, Sara P, Margriet JVB, Heidi VDR, Kristien B, et al. (2007) Silane ligand exchange to make hydrophobic superparamagnetic nanoparticles water-dispersible. *Chem Mater* 19: 1821-1831.
  51. Itoh H, Sugimoto T (2003) Systematic control of size, shape, structure, and magnetic properties of uniform magnetite and maghemite particles. *J Colloid Interf Sci* 265(2): 283-295.
  52. Weissleder R, Elizondo G, Wittenberg J, Rabito CA, Bengele HH, et al. (1990) Ultrasmall superparamagnetic iron oxide: characterization of a new class of contrast agents for MR imaging. *Radiology* 175(2): 489-93.
  53. Tassa C, Shaw SY, Weissleder R (2011) Dextran-Coated Iron Oxide Nanoparticles: A Versatile Platform for Targeted Molecular Imaging, Molecular Diagnostics, and Therapy. *Acc Chem Res* 44 (10): 842-852.
  54. Josephson L, Perez JM, Weissleder R (2001) Magnetic nanosensors for the detection of oligonucleotide sequences. *Angew Chem, Int Ed* 40: 3204-3206.
  55. Perez JM, Josephson L, Loughlin O'T, Högemann D, Weissleder R (2002) Magnetic relaxation switches capable of sensing molecular interactions. *Nat Biotechnol* 20(8): 816-820.
  56. Lewin M, Carlesso N, Tung CH, Tang XW, Cory D, et al. (2000) Tat peptide-derivatized magnetic nanoparticles allow in vivo tracking and recovery of progenitor cells. *Nat Biotechnol* 18(4): 410-414.
  57. Jaffer FA, Nahrendorf M, Sosnovik D, Kelly KA, Aikawa E, et al. (2006) Cellular imaging of inflammation in atherosclerosis using magnetofluorescent nanomaterials. *Mol Imaging* 5(2): 85-92.
  58. Lee H, Sun E, Ham D, Weissleder R (2008) Chip-NMR biosensor for detection and molecular analysis of cells. *Nat Med* 14(8): 869-874.
  59. Hahn PF, Stark DD, Lewis JM, Saini S, Elizondo G, et al. (1990) First clinical trial of a new superparamagnetic iron oxide for use as an oral gastrointestinal contrast agent in MR imaging. *Radiology* 175(3): 695-700.
  60. Smith EA, Chen W (2008) How to prevent the loss of surface functionality derived from aminosilanes. *Langmuir* 24(21): 12405-12409.
  61. Yamaura M, Camilo RL, Sampaio LC, Macêdo MA, Nakamura M, et al. (2004) Preparation and characterization of (3-aminopropyl) triethoxysilane-coated magnetite nanoparticles. *J Magn Magn Mater* 279: 210-217.
  62. Bruce IJ, Sen T (2005) Surface modification of magnetic nanoparticles with alkoxysilanes and their application in magnetic bioseparations. *Langmuir* 21(15): 7029-7035.
  63. Jung CW (1995) Surface properties of superparamagnetic iron oxide MR contrast agents: Ferumoxides, ferumoxtran, ferumoxsil. *Magn Reson Imaging* 13(5): 675-691.
  64. Jung CW, Jacobs P (1995) Physical and chemical properties of superparamagnetic iron oxide MR contrast agents: Ferumoxides, ferumoxtran, ferumoxsil. *Magn Reson Imaging* 13(5): 661-674.
  65. Kwon SG, Hyeon T (2011) Formation mechanisms of uniform nanocrystals via hot-injection and heat-up methods. *Small* 7(19): 2685-2702.
  66. Herman DA, Ferguson P, Cheong S, Hermans IF, Ruck BJ, et al. (2011) Hot-injection synthesis of iron/iron oxide core/shell nanoparticles for T2 contrast enhancement in magnetic resonance imaging. *Chem Commun* 47(32): 9221-9223.
  67. Park J, Joo J, Kwon SG, Jang Y, Hyeon T (2007) Synthesis of monodisperse spherical nanocrystals. *Angew Chem Int Ed* 46(25): 4630-4660.
  68. Cheon J, Kang NJ, Lee SM, Lee JH, Yoon JH, Oh SJ (2004) Shape Evolution of Single-Crystalline Iron Oxide Nanocrystals. *J Am Chem Soc* 126(7): 1950-1951.
  69. Nikhil RJ, Yongfen C, Xiaogang P (2004) Size- and Shape-Controlled Magnetic (Cr, Mn, Fe, Co, Ni) Oxide Nanocrystals via a Simple and General Approach. *Chem Mater* 16(20): 3931-3935.
  70. Frey NA, Peng S, Cheng K, Sun S (2009) Magnetic nanoparticles: synthesis, functionalization, and applications in bioimaging and magnetic energy storage. *Chem Soc Rev* 38(9): 2532-2542.
  71. Murray CB, Kagan CR, Bawendi MG (2000) Synthesis and characterization of monodisperse nanocrystals and close-packed nanocrystal assemblies. *Annual Review of Materials Science* 30: 545-610.
  72. Victor KLM, Robert HD (1950) Theory, production and mechanism of formation of monodispersed hydrosols. *J Am Chem Soc* 72(11): 4847-4854.
  73. Lee Y, Lee J, Bae CJ, Park JG, Noh HJ, et al. (2005) Large-scale synthesis of uniform and crystalline magnetite nanoparticles using reverse

- micelles as nanoreactors under reflux conditions. *Advanced Functional Materials* 15: 503-509.
74. Gittins DI, Caruso F (2001) Spontaneous phase transfer of nanoparticulate metals from organic to aqueous media. *Angew Chem, Int Ed* 40(16): 3001-3004.
  75. Zhou Z, Zhu X, D Wu, Q Chen, D Huang, et al. (2015) Anisotropic Shaped Iron Oxide Nanostructures: Controlled Synthesis and Proton Relaxation Shortening Effects. *Chem Mater* 27: 3505-3515.
  76. Zhen L, Hui C, Haobo B, Mingyuan G (2004) One-Pot Reaction to Synthesize Water-Soluble Magnetite Nanocrystals. *American Chemical Society* 16(8): 1391-1393.
  77. Li Z, Sun Q, Gao M (2005) Preparation of water-soluble magnetite nanocrystals from hydrated ferric salts in 2-pyrrolidone: Mechanism leading to Fe<sub>3</sub>O<sub>4</sub>. *Angew Chem Int Ed* 44(1): 123-126.
  78. Ge J, Hu Y, Biasini M, Beyermann WP, Yin Y (2007) Superparamagnetic Magnetite Colloidal Nanocrystal Clusters. *Angew Chem Int Ed* 46(23): 4342-4345.
  79. Ge J, Hu Y, Biasini M, Dong C, Guo J, et al. (2007) One-step synthesis of highly water-soluble magnetite colloidal nanocrystals. *Chemistry* 13(25): 7153-7161.
  80. Kheireddine El-B, Rabih OAI-K, Muhanna KAI-M, Hassan MB, Abdulaziz IAI-R, et al. (2015) Ultra-Small Fatty Acid-Stabilized Magnetite Nanocolloids Synthesized by In Situ Hydrolytic Precipitation. *Journal of Nanomaterials* pp11.
  81. Sinha R, Kim GJ, Nie S, Shin DM (2006) Nanotechnology in cancer therapeutics: bioconjugated nanoparticles for drug delivery. *Mol Cancer Ther* 5(8): 1909-1917.
  82. Rejman J, Oberle V, Zuhorn IS, Hoekstra D (2004) Size-dependent internalization of particles via the pathways of clathrin- and caveolae-mediated endocytosis. *Biochem J* 377(1):159-169.
  83. Mura S, Nicolas J, Couvreur P (2013) Stimuli-responsive nanocarriers for drug delivery. *Nat Mater* 12(11): 991-1003.
  84. Cheng R, Meng F, Deng C, Klok HA, Zhong Z (2013) Dual and multi-stimuli responsive polymeric nanoparticles for programmed site-specific drug delivery. *Biomaterials* 34(14): 3647-3657.
  85. Boubbou El-K, Ali R, Bahhari HM, AlSaad KO, Nehdi A, et al. (2016) Magnetic Fluorescent Nanoformulation for Intracellular Drug Delivery to Human Breast Cancer, Primary Tumors, and Tumor Biopsies: Beyond Targeting Expectations. *Bioconjugate Chem* 27(6): 1471-1483.
  86. Huang J, Li Y, Orza A, Lu Q, Guo P, Wang L, et al. (2016) Magnetic Nanoparticle Facilitated Drug Delivery for Cancer Therapy with Targeted and Image-Guided Approaches. *Adv Funct Mater* 26(22): 3818-3836.
  87. Kim J, Piao Y, Hyeon T (2009) Multifunctional nanostructured materials for multimodal imaging, and simultaneous imaging and therapy. *Chem Soc Rev* 38(2): 372-390.
  88. Lee JH, Huh YM, Jun YW, Seo JW, Jang JT, et al. (2007) Artificially engineered magnetic nanoparticles for ultra-sensitive molecular imaging. *Nat Med* 13(1): 95-99.
  89. Jarzyna PA, Gianella A, Skajaa T, Knudsen G, Deddens LH, et al. (2010) Multifunctional imaging nanoprobe. *Wiley Interdiscip Rev Nanomed Nanobiotechnol* 2(2): 138-150.
  90. Josephson L, Kircher MF, Mahmood U, Tang Y, Weissleder R (2002) Near-Infrared Fluorescent Nanoparticles as Combined MR/Optical Imaging Probes. *Bioconjugate Chem* 13(3): 554-560.
  91. Moore A, Medarova Z, Potthast A, Dai G (2004) In vivo targeting of underglycosylated MUC-1 tumor antigen using a multimodal imaging probe. *Cancer Res* 64(5): 1821-1827.
  92. Pittet MJ, Swirski FK, Reynolds F, Josephson L, Weissleder R (2006) Labeling of immune cells for in vivo imaging using magnetofluorescent nanoparticles. *Nat Protoc* 1(1): 73-79.
  93. Nahrendorf M, Zhang H, Hembrador S, Panizzi P, Sosnovik DE, et al. (2008) Nanoparticle PET-CT imaging of macrophages in inflammatory atherosclerosis. *Circulation* 117(3): 379-387.
  94. M Nahrendorf, E Keliher, B Marinelli, Waterman P, Feruglio PF, et al. (2010) Hybrid PET -optical imaging using targeted probes. *Proc Natl Acad Sci* 107: 7910-7915.
  95. Lee JH, Lee K, Moon SH, Lee Y, Park TG, et al. (2009) All-in-One Target-Cell-Specific Magnetic Nanoparticles for Simultaneous Molecular Imaging and siRNA Delivery. *Angew Chem, Int Ed* 48(23): 4174-41279.
  96. Datta A, Raymond KN (2009) Gd-hydroxypyridinone (HOPO)-based high-relaxivity magnetic resonance imaging (MRI) contrast agents. *Acc Chem Res* 42(7): 938-947.
  97. Bae KH, Kim YB, Lee Y, Hwang J, Park H, et al. (2010) Bioinspired Synthesis and Characterization of Gadolinium-Labeled Magnetite Nanoparticles for Dual Contrast T1- and T2-Weighted Magnetic Resonance Imaging. *Bioconjugate Chem* 21(3): 505-512.
  98. Amstad E, Gillich T, Bilecka I, Textor M, Reimhult E (2009) Ultrastable Iron Oxide Nanoparticle Colloidal Suspensions Using Dispersants with Catechol-Derived Anchor Groups. *Nano Letters* 9(12): 4042-4048.
  99. Jianhua S, Yunfeng L, Yihua Z, Xiaoling Y, Xiuzhong Y, et al. (2015) Multifunctional gadolinium-labeled silica-coated Fe<sub>3</sub>O<sub>4</sub> and CuInS<sub>2</sub> nanoparticles as a platform for in vivo tri-modality magnetic resonance and fluorescence imaging. *J Mater Chem B* 3: 2873-2882.



This work is licensed under Creative Commons Attribution 4.0 License  
DOI: [10.19080/GJN.2017.01.555571](https://doi.org/10.19080/GJN.2017.01.555571)

**Your next submission with JuniperPublishers  
will reach you the below assets**

- Quality Editorial service
- Swift Peer Review
- Reprints availability
- E-prints Service
- Manuscript Podcast for convenient understanding
- Global attainment for your research
- Manuscript accessibility in different formats  
( Pdf, E-pub, Full Text, Audio)
- Unceasing customer service

**Track the below URL for one-step submission**

<https://juniperpublishers.com/submit-manuscript.php>